

# Design of Silicon Hetero-Interface Photodetectors

Weishu Wu, Aaron R. Hawkins, and John E. Bowers

**Abstract**— In a silicon hetero-interface photodetector, Si is used as the multiplication material to provide avalanche gain, while InGaAs is used as the absorption material. High quantum efficiency, high gain-bandwidth product, and low noise detection of wavelengths between 1.0 and 1.6  $\mu\text{m}$  can be achieved in this way. We derive expressions for the frequency response for these detectors, present possible design variations, and analyze their performance. The effects of parasitics, transit time, and RC roll-off on frequency response are investigated and the 3-dB bandwidth and gain bandwidth product are calculated. Particular attention is paid to a 10 Gbit/s APD and we show that that a 3-dB bandwidth of 10 GHz and a gain-bandwidth product in excess of 400 GHz should be possible.

**Index Terms**— Avalanche photodiodes, high-speed devices, optoelectronic devices, photodetectors, semiconductor devices.

## I. INTRODUCTION

HIGH GAIN, large bandwidth, and low-noise avalanche photodetectors (APD's) are increasingly attractive for use in high bit-rate optical communication systems because of the internal gain provided by APD's [1]–[3]. Silicon APD's are well known for their low excess noise and large gain-bandwidth product due to the large asymmetry of electron and hole ionization coefficients [4]. However, the quantum efficiency of Si APD's for light wavelengths between 1.3–1.6  $\mu\text{m}$  regime is negligible, making them unusable for modern optical communication systems. On the other hand, InGaAs has a much higher absorption coefficient at 1.3–1.6  $\mu\text{m}$  than Si [5], resulting in a much larger quantum efficiency. InGaAs/InP APD's [6]–[8] with separate absorption and multiplication (SAM) have good quantum efficiency at 1.3–1.6  $\mu\text{m}$ , but the gain-bandwidth product is much smaller than that of Si-APD's due to the small asymmetry of ionization coefficients in InP. A gain-bandwidth product of 150 GHz has been demonstrated in InGaAs/AlGaAs superlattice based APD's [9]. However, the achievable gain-bandwidth product is smaller than that of Si-APD's. Further, the voltage and temperature sensitivity of Si-APD's is much better than that of InP or superlattice APD's. Therefore, it is beneficial to combine the desirable properties of both Si and InGaAs.

The first Si/InGaAs APD, a silicon hetero-interface photodetector (SHIP), was fabricated using wafer fusion [10], and a gain-bandwidth product of 81 GHz [11] was obtained. The SHIP detector is shown schematically in Fig. 1. It consists of the following layers. An  $n^+$  Si substrate, with an  $n^-$  Si epitaxial layer grown on it; a p-InGaAs layer as the absorption

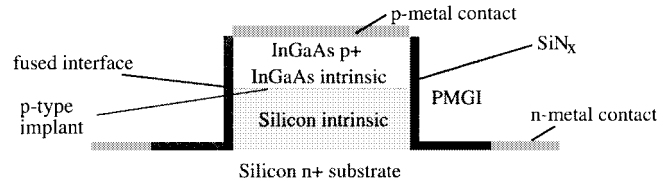


Fig. 1. Schematic drawing of the structure of a SHIP detector.

layer; and a  $p^+$  InGaAs layer for p-contact. Near the interface of Si and InGaAs, p-dopants are implanted to adjust the electric field in Si so that avalanche multiplication can be sustained in Si and at the same time, the electric field in the absorption region is kept at a low level such that no multiplication takes place in the InGaAs layer. For SHIP detectors currently under fabrication, there are no grading layers between the Si and InGaAs layers. Our devices are back-illuminated through the Si substrate but front illumination is possible for UV to IR wavelengths. Important parameters of performance include the 3-dB bandwidth at small gain regime and the gain-bandwidth product in the high gain regime. At small gains, the limitation on the 3-dB bandwidth of a SHIP detector is very similar to that on a PIN detector [5]. In this paper, we analyze the performance of SHIP APD's using an exact expression to the frequency response of SHIP APD's based on Hollenhorst's method [12]. The effects of parasitics, transit time, and avalanche buildup time are also considered. Design curves for different thicknesses of multiplication layers and absorption layers are presented. Experimental results based on these design are also presented.

## II. THEORY

In this section, the exact solution to the frequency response of SHIP APD's will be derived. Important performance figures, such as 3 dB bandwidth and gain-bandwidth product, can be obtained by calculating the frequency response. Analytical expressions of frequency response for SAM-APD's were first presented by Campbell *et al.* [13]. In deriving their analytic expressions, they assumed that all the multiplication takes place effectively at a plane near the peak electric field. They further assumed that the multiplication layer was so thin that this effective multiplication plane was at the edge of the depletion layer. Recently, we presented a theory on the frequency response of SAM-APD's [14]. The assumption that the effective multiplication plane is located at the edge of the depletion layer was eliminated. Depending on the electric field profile in the multiplication layer, the effective plane of avalanche multiplication can be anywhere inside the multiplication layer. For nonuniform electric field profiles,

Manuscript received September 16, 1996; revised January 13, 1997. This work was supported by ARPA and Rome Labs.

The authors are with the Electrical and Computer Engineering Department, University of California at Santa Barbara, Santa Barbara, CA 93106 USA.

Publisher Item Identifier S 0733-8724(97)06055-6.

their effect can be taken into account by properly choosing the position of the effective multiplication layer. In this way, analytic expressions for both time and frequency response can be obtained. However, for SAM-APD's with a few layers and a uniform avalanche electric field profile, the approach developed by Hollenhorst [12] (and independently by Kahraman *et al.* in a similar method [15]) is a better way to calculate their frequency response. Although the approach is mathematically more complicated than the "effective multiplication plane" approach, the assumption that all multiplication takes place at the same plane has been eliminated. Therefore, the avalanche process is more precisely described and the quantities such as gain and avalanche buildup time are inherently taken into account in Hollenhorst's approach. For the SHIP APD's shown in Fig. 1, the depletion region contains only two layers and the electric field is almost uniform inside each layer. Therefore, it is possible to obtain analytic expression for the frequency response using Hollenhorst's approach. The effect of grading layers (if any) can be easily incorporated into the formula for future SHIP detectors.

Using Hollenhorst's notation [12], the current density components at a certain frequency,  $\omega$ , entering and leaving a given layer (terminal currents) are related by the following equation:

$$\begin{bmatrix} J_{p1} \\ J_{n1} \end{bmatrix} = \begin{bmatrix} T_{pp} & T_{pn} \\ T_{np} & T_{nn} \end{bmatrix} \begin{bmatrix} J_{p0} \\ J_{n0} \end{bmatrix} + \begin{bmatrix} S_p \\ S_n \end{bmatrix} \quad (1a)$$

or in a simpler form

$$\vec{J}_1 = \mathbf{T}\vec{J}_0 + \vec{S} \quad (1b)$$

where the subscripts "p" and "n" represent the hole component and electron component, respectively.  $\mathbf{T}$  is the current transfer matrix which varies with different layers, and  $\vec{S}$  is the source current vector, representing the current components due to optical sources [12]. The corresponding electrode current densities due to  $\vec{J}_0$  is given by

$$I(\omega) = \frac{1}{w_d} (\vec{U} \cdot \vec{J}_0 + V) \quad (2)$$

where  $w_d$  is the thickness of the depletion layer,  $\vec{U} = \begin{bmatrix} U_p \\ U_n \end{bmatrix}$  is the electrode response determining the proportionality between the left-hand terminal currents and the electrode current, and  $V$  is the contribution from the optical source [12] (note that in [12],  $\vec{E}$  and  $D$  are used instead of  $\vec{U}$  and  $V$ ). Detailed expressions of  $\mathbf{T}$ ,  $\vec{S}$ ,  $\vec{U}$ , and  $V$  for several most-frequently used layers have been derived in [12], under the assumption that the holes are propagating in the  $+x$  direction and the electrons are propagating in the  $-x$  direction, as shown in Fig. 2(a). For a SHIP detector with two layers as shown in Fig. 2(b), the quantities relating  $\begin{bmatrix} J_{p0} \\ J_{n0} \end{bmatrix}$  and  $\begin{bmatrix} J_{p2} \\ J_{n2} \end{bmatrix}$  are given by, according to the composition rules (see [12, eq. (8)])

$$\begin{aligned} \mathbf{T} &= \mathbf{T}^a \mathbf{T}^m \\ \vec{S} &= \vec{S}^a \quad (\vec{S}^m = 0) \\ \vec{U} &= (\vec{U}^m) + (\vec{U}^a) \mathbf{T}^m \\ V &= V^a \quad (V^m = 0), \end{aligned} \quad (3)$$

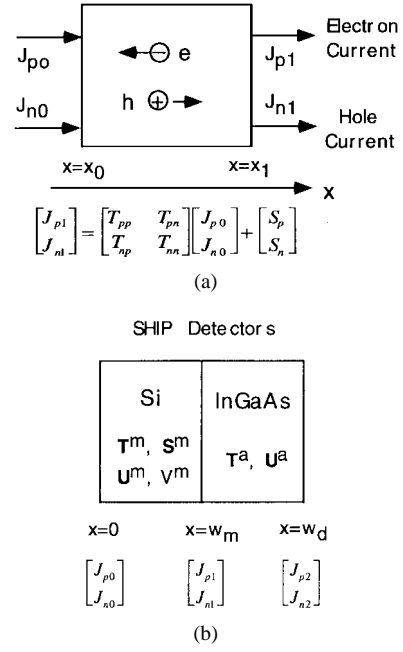


Fig. 2. Electron and hole currents for (a) a uniform layer and (b) a two-layer SHIP APD's.

The quantities  $\mathbf{T}$ ,  $\vec{S}$ ,  $\vec{U}$ , and  $V$  are defined for the purpose that these quantities can easily be calculated for multilayer structures based on the composition rules. Practically, however, we need to express  $I(\omega)$  with the injected currents,  $\vec{J}_{in} = \begin{bmatrix} J_{p0} \\ J_{n0} \end{bmatrix}$ . Therefore, (2) must be rewritten in the form of

$$I(\omega) = \frac{1}{w_d} (\vec{\rho} \cdot \vec{J}_{in} + \delta) \quad (4)$$

so that contribution to the electrode current from the injected currents and/or optical sources can be calculated.

Given (1)–(3), it is straightforward to solve  $I(\omega)$  in the form of (4). For APD's without injected holes and electrons, the electrode current due to photon absorption  $\delta/w_d$  can be solved as

$$I(\omega) = \frac{1}{w_d} \left[ \left( V^a - \frac{U_n^a S_n^a}{T_{nn}^a} \right) - \frac{S_n^a}{T_{nn}^a} \left( \frac{U_n^m}{T_{nn}^m} + U_p^a \frac{T_{pn}^m}{T_{nn}^m} \right) \right] \quad (5)$$

The quantities contained in the bracket are given in [12]. The superscripts  $a$  and  $m$  denote absorption and multiplication layers, respectively. It can be shown that dc electrode current  $I(0)$  is simply  $(eP_0/h\nu)M_e[1 - \exp(-\alpha_a w_a)]$  where  $e$  is the electronic charge,  $P_0$  is the energy of the optical impulse,  $h\nu$  is the photon energy,  $\alpha_a$  is the absorption coefficient. By including the parasitic effects, the frequency response of the APD is given by

$$\text{F.R.} \equiv \frac{1}{1 - \omega^2 LC + j\omega RC} \frac{I(\omega)}{I(0)} \quad (6)$$

where  $L$  is the parasitic inductance,  $C$  is the total capacitance,  $R$  is the sum of the series resistance and the load resistance. Equations (5) and (6) can be used to calculate the 3-dB bandwidth and gain-bandwidth product for a SHIP detector.

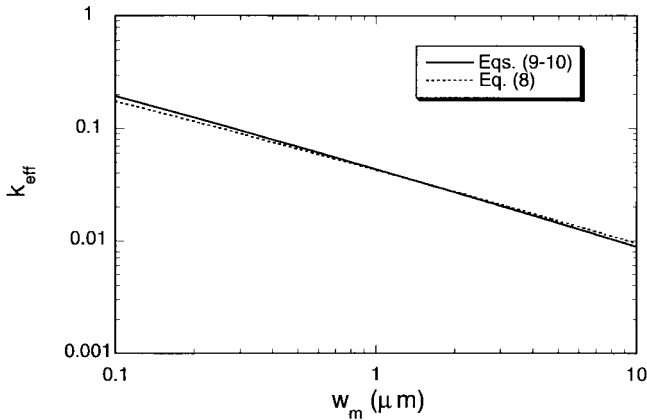


Fig. 3. Ionization coefficients as functions of  $w_m$  using (9), (10), and (8) (dotted line).

### III. OPERATING VOLTAGE OF A SHIP DETECTOR

When designing SHIP detectors, it is very important to have accurate knowledge of the ionization coefficients of Si. It is well known that multiplication gain, avalanche buildup time, and noise of an APD are strongly dependent on the ionization coefficients of the material used for avalanche multiplication. Given an electron ionization coefficient  $\alpha$  and a hole ionization coefficient  $\beta$  for a uniform electric field profile, the multiplication gain for electrons  $M_e$  can be expressed as [16]

$$M_e = \frac{(\alpha - \beta) \exp[(\alpha - \beta)w_m]}{\alpha - \beta \exp[(\alpha - \beta)w_m]} \quad (7)$$

where  $w_m$  is the thickness of the multiplication layer.

It has been shown that a small  $k_{\text{eff}}$ , defined by the ratio of the smaller ionization coefficient to the larger one (hence it is always smaller than 1), will result in a large gain-bandwidth product [4], [17], [18] and a small excess noise figure [19] for an APD. Among several most frequently used materials for avalanche multiplication [20]–[23], Si is by far the most promising material due to its smallest ratio of the electron and hole ionization coefficients. Since the ionization coefficients play such an important role in designing APD's, many attempts have been made to precisely determine the ionization coefficients of Si as functions of electric field [16], [20], [24]. Unfortunately the measured results do not agree with each other, and the resultant  $k_{\text{eff}}$  does not agree with the experimental results obtained by Kaneda *et al.* [25] based on the measurement of the excess noise of reach-through Si-APD's [26]. According to the measurements by Kaneda [25], the ratio of the ionization coefficients of silicon as a function of the multiplication layer thickness can be expressed as

$$k_{\text{eff}}(w_m) = 0.22k_{\text{Grant}}(w_m) \quad (8)$$

where  $k_{\text{Grant}}(w_m)$  is the ratio of the ionization coefficients near breakdown, using Grant's ionization coefficients, for a given multiplication layer thickness. Due to the similarity in electric field profiles in the multiplication region between the reach-through APD's and SAM-APD's, the values of  $k_{\text{eff}}$  as a

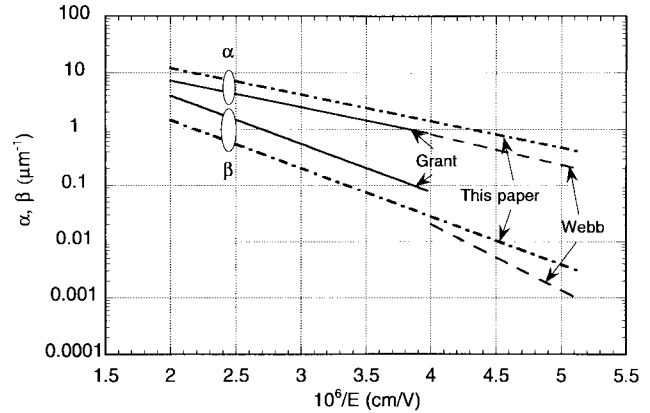


Fig. 4. Ionization coefficients in Si as functions of electric field.

function of  $w_m$  obtained in this way should be more accurate and more suitable to SAM-APD's because those values were obtained at similar high electric fields in multiplication layers of similar thicknesses.

Kaneda's data only gives the best approximation on the ratio of the coefficients near breakdown voltage for a given thickness of the multiplication layer. It is necessary, however, to know the individual ionization coefficients to calculate the required electric field at arbitrary gains for a given multiplication layer thickness. More specifically, we need to know the coefficients as functions of the electric field. To this end, we use the following empirical expressions for the ionization coefficients:

$$\alpha(E) = 104 \exp(-1.08 \times 10^6/E) \quad (9)$$

$$\beta(E) = 77 \exp(-1.97 \times 10^6/E) \quad (10)$$

where  $E$  is the electric field in units of  $\text{kV/cm}$ . Using these equations, the dependence of  $k_{\text{eff}}$  on  $w_m$  at breakdown is plotted in Fig. 3. We can see that the ratio given by (9) and (10) (solid line) is very close to the values given by (8) which is based on Kaneda's experimental results. The ionization coefficients given by (9) and (10) are plotted in Fig. 4 together with that given by Grant [16] and Webb [20]. The coefficients given by (9) and (10) are the best estimate based on [16], [20], [24], [25].

Giving the ionization coefficients as of (9) and (10), we can now calculate the required electric fields as functions of the avalanche gain for various thicknesses of the multiplication layer. The dependence of the required electric field on the avalanche gain is shown in Fig. 5 for a  $1 \mu\text{m}$  multiplication layer. We can see that when gain increases slowly as the increase of the electric field until  $M_e > 100$ . Therefore when the gain is smaller than 100, we can control the gain by adjusting the applied voltage. The dependence of the required electric field for infinite gain (breakdown), as well as the corresponding voltage across the multiplication layer, on the layer thickness is plotted in Fig. 6. The actual operating voltage is the voltage shown in Fig. 6 plus the voltage needed to deplete the absorption layer, which depends on the doping level of the absorption layer.

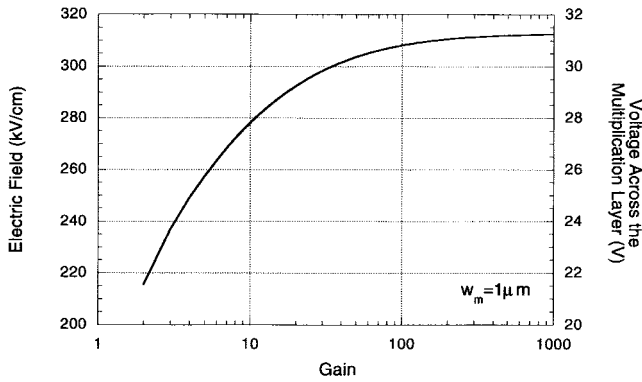


Fig. 5. Dependence of the required electric field and the voltage across the multiplication layer on the avalanche gain for  $w_m = 1 \mu\text{m}$ , assuming uniform electric field.

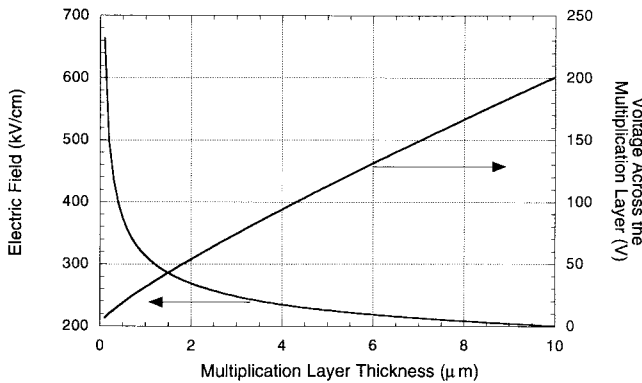


Fig. 6. Dependence of the required electric field and the corresponding voltage on the thickness of the multiplication layer near breakdown.

#### IV. BANDWIDTH AND QUANTUM EFFICIENCY OF SHIP DETECTORS

The speed of an APD is an important parameter, especially in optical communications applications. The major limitations on the speed of a SHIP detector include 1) the electron and hole transit time, 2) the avalanche buildup time  $M_e\tau_e$ , and 3) the time it takes to charge and discharge the inherent capacitance of the p-n junction as well as any parasitic capacitance, i.e., the RC effect. The transit time plays an important role in the speed of APD's due to the contribution from the secondary charges generated by avalanche multiplication. For SHIP detectors, the secondary holes need to drift through the absorption layer after the primary electrons drift through it, thus nearly doubling the transit time needed for a PIN detector with the same dimension.

Another consideration on the speed of an APD is the avalanche buildup time. In the high gain regime, the speed of an APD is mainly limited by this parameter. The gain-bandwidth product of an APD is therefore determined by the avalanche buildup time through the relationship  $GB = 1/2\pi\tau_e$ . These considerations on the transit time and avalanche buildup time suggest that very thin absorption layers and multiplication layers are desirable to achieve high frequency response. However, as the absorption and/or multiplication layer is decreased, the capacitance is increased. As a result, the RC time constant will be significantly increased. For SHIP

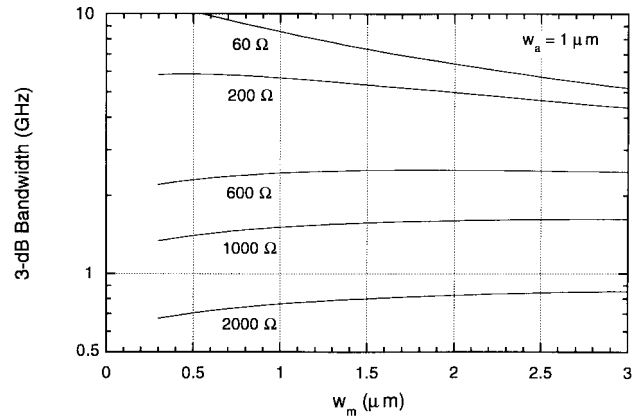


Fig. 7. The dependence of 3-dB bandwidth on the multiplication layer thickness for different values of resistance at  $M_e = 10$ .

TABLE I  
PARAMETERS USED IN THE CALCULATION

$C_{pad}$	0.08 pF
$A$	$415 \mu\text{m}^2$
$\epsilon_a$	14.1
$\epsilon_m$	11.7
$L$	0
$v_n^a$	$7.0 \times 10^6 \text{ cm/s}$
$v_p^a$	$4.8 \times 10^6 \text{ cm/s}$
$v_n^m$	$1.05 \times 10^7 \text{ cm/s}$
$v_p^m$	$7.5 \times 10^6 \text{ cm/s}$
$\alpha_a$	$1.15 \mu\text{m}^{-1}$

detectors, the resistance is the sum of the load resistance and the series resistance of the APD's, while the capacitance can be expressed as

$$C = C_{pad} + \frac{\frac{1}{4}\epsilon_0\pi D^2}{\frac{w_a}{\epsilon_a} + \frac{w_m}{\epsilon_m}} \quad (11)$$

where  $C_{pad}$  is capacitance due to bonding pads,  $\epsilon_0$ ,  $\epsilon_m$ , and  $\epsilon_a$  are the dielectric constants in vacuum, Si, and InGaAs, respectively,  $D$  is the diameter of the active region of the APD, and  $w_a$  and  $w_m$  are the absorption layer thickness and the multiplication layer thickness, respectively. The relative importance of the RC time limit and transit time limit depends, to a large extent, on the resistance and/or the area of the APD. This is illustrated in Fig. 7, which shows the dependence of 3 dB bandwidth at a gain of ten on the multiplication layer thickness for several values of resistance for  $w_a = 1 \mu\text{m}$  and a fixed active area of  $415 \mu\text{m}^2$  ( $D = 23 \mu\text{m}$ ). The parameters used in this calculation are listed in Table I. In general, for a given  $w_m$ , as the resistance increases the bandwidth decreases. With a fixed value of the resistance that is much smaller than  $600 \Omega$ , the bandwidth increases as the multiplication layer

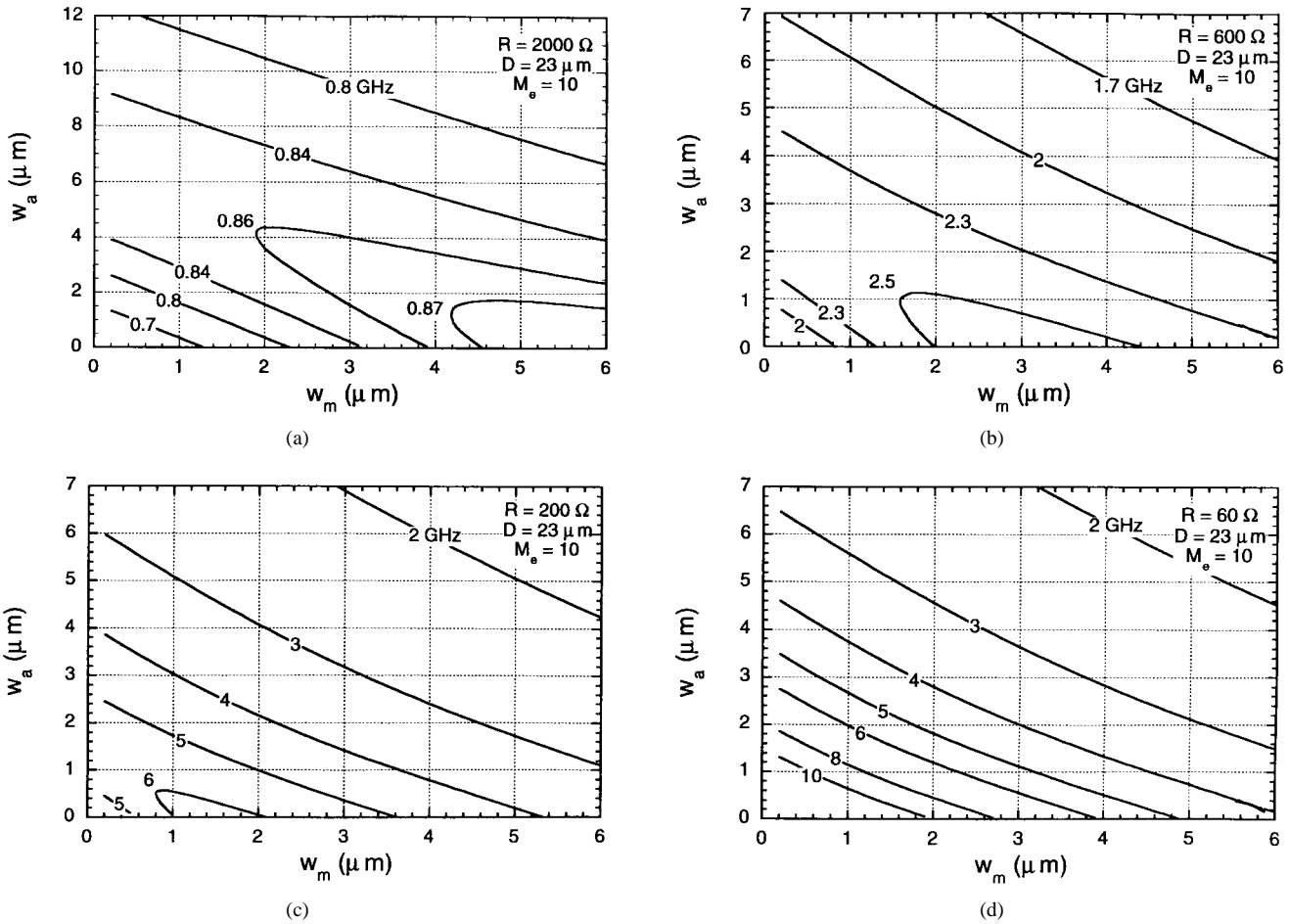


Fig. 8. Contour plot of constant 3-dB bandwidth at a gain of ten in  $w_m - w_a$  plane for (a)  $R = 2000 \Omega$ , (b)  $R = 600 \Omega$ , (c)  $R = 200 \Omega$ , and (d)  $R = 60 \Omega$ . The area of the SHIP detector is  $415 \mu\text{m}^2$ , which corresponds to a diameter of  $23 \mu\text{m}$ .

thickness decreases, indicating that the transit time is the main limitation imposed on the speed of the detector. However, when the resistance approaches  $600 \Omega$ , the 3-dB bandwidth changes only slightly over a wide range of multiplication layer thickness, indicating that the effects of RC roll-off and transit time cancel each other. If the resistance further increases, the bandwidth finally decreases by decreasing the thickness of the multiplication layer, indicating that the RC roll-off prevails.

In principle, the bandwidth can be further increased by decreasing the thickness of the absorption layer. This is shown in Fig. 8, where contours of constant bandwidth at a gain of ten are plotted in the  $w_m - w_a$  plane. The shape of the contour is determined by the drift velocities of hole and electrons and the dielectric constants of both layers. When the resistance is high, each contour corresponding to a high bandwidth is usually composed of two branches: one corresponds to the transit time limit and the other corresponds to the RC roll-off limit. On the other hand, when the resistance is small, the branch corresponding to the RC limit will vanish and higher bandwidth can be achieved by decreasing the thickness of the absorption and/or multiplication layers, as shown in Fig. 8(d) for  $R = 60 \Omega$ . The highest bandwidth achievable for a  $60 \Omega$  resistance is around 13 GHz.

If the absorption layer is too thin, the quantum efficiency will be significantly decreased. Therefore, there is a tradeoff

between the quantum efficiency and the transit time when choosing the thickness of the absorption layer. Note that the quantum efficiency is related to the thickness of the absorption layer according to

$$\eta = (1 - R_F)(1 - \exp(-\alpha_a w_a)) \tag{12}$$

where  $R$  is the Fresnel reflectivity and is the absorption coefficient. The gain-bandwidth product of the APD at high gains is related to  $w_m$  by [19]

$$GB = \frac{1}{\pi k k_{\text{eff}}(w_m/v_p + w_m/v_n)} \tag{13}$$

and so the contours can also be plotted in  $GB - \eta$  plane, as shown in Fig. 9(a)–(d).

Equation (13) implies that the gain-bandwidth product at high gains is a constant for a given thickness of the multiplication layer. This is true because the bandwidth of an APD is mainly limited by the multiplication gain  $M_e$  at high gains. The dependence of the resultant 3-dB bandwidth on the avalanche gain is shown in Fig. 10 where the absorption layer thickness is fixed at  $1 \mu\text{m}$ . We can see that when the gain is large enough, the gain-bandwidth product is indeed a constant, which is in agreement with (13).

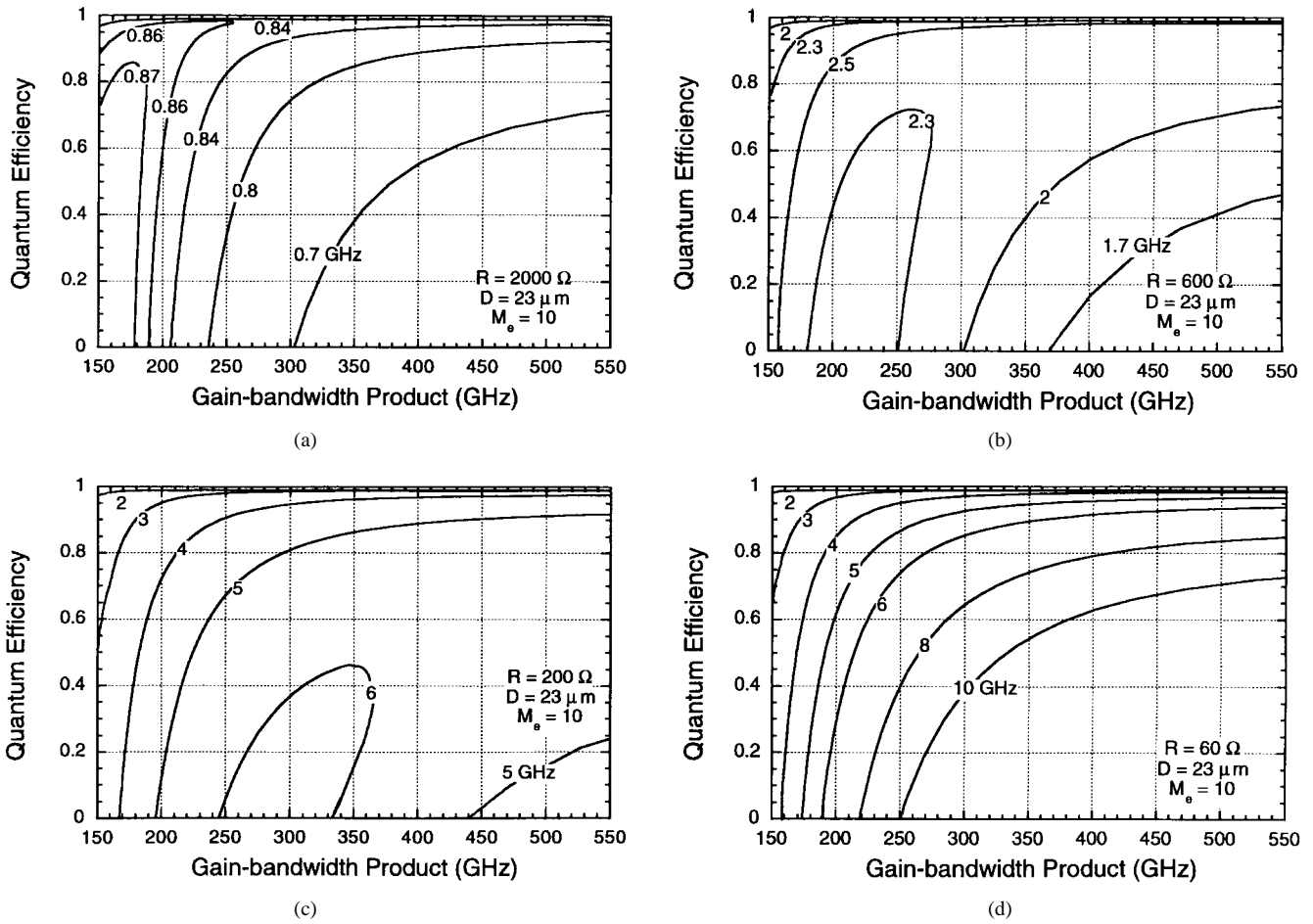


Fig. 9. Contour plot of constant 3-dB bandwidth at a gain of ten in  $GB - \eta$  plane for an AR-coated SHIP detector of active area of  $415 \mu\text{m}^2$ .

## V. MEASUREMENTS

The construction of SHIP detectors (Fig. 1) involves direct wafer fusion of an InGaAs epitaxial layer with a Si substrate. This process is done in an  $\text{H}_2$  atmosphere at a temperature of  $650^\circ\text{C}$ , near the epitaxial growth temperature of the InGaAs. Details of the fabrication are given in [27]. To determine the quality of the hetero-interface between Si and InGaAs we have measured detector quantum efficiencies and made TEM scans. Quantum efficiency measurements indicate nearly ideal electron transport of photo-generated electrons from InGaAs into Si. This indicates the absence of carrier traps or large conduction band discontinuities between the materials. TEM scans indicate that edge dislocations form at the boundary of the heterointerface to accommodate the lattice mismatch between Si and InGaAs [11]. These defects are isolated at the interface, however, and do not propagate up into the crystal structure of either material. Further study of carrier transport across the junction as well as measurements of the conduction band offsets will be done in the future.

The 3-dB bandwidths of SHIP detectors at different gains have been measured. For a SHIP APD with  $w_a = 1 \mu\text{m}$  and  $w_m = 2.5 \mu\text{m}$ , the measured results are shown in Fig. 11 together with the theoretical calculations. The resistance of the APD was  $R = 2020 \Omega$  and the capacitance was  $C = 0.1 \text{ pF}$ . Due to the large contact resistance, the bandwidths at small

gains (about 0.78 GHz) were mainly limited by the large RC time constant. The maximum measured gain-bandwidth product for that InGaAs/Si detector was 81 GHz, limited by the thick multiplication layer. For a recently designed SHIP APD, we reduced the multiplication layer thickness to  $0.6 \mu\text{m}$ . At the same time, the ohmic contact was also improved. As a result, we obtained a bandwidth of 13 GHz and a gain-bandwidth product of 315 GHz [27], as shown in Fig. 12.

From the above discussion, we can conclude that for a SHIP detector with very small resistance, the RC limit is usually not a very significant factor. Therefore, a small thickness of the depletion layer (hence a small transit time) is desirable. The minimum thickness for the absorption layer is therefore determined by the requirement of quantum efficiency. On the other hand, if the multiplication layer is made thinner and thinner, the required electric field to achieve high avalanche gain will be higher and higher. Therefore, the minimum thickness of the multiplication layer is limited by the allowable dark current and sustainable electric field, which are, in turn, dependent on the tunneling effect and the doping level in the multiplication material. In addition, nonlocal effects such as the dead space associated with avalanche in a thin layer will no longer be negligible. Note that if the area of a SHIP detector is changed, the effect of this change is equivalent to a proportional change in the resistance. Hence, the Fig. 8 and Fig. 9 are also useful for a fixed resistance but various active areas.

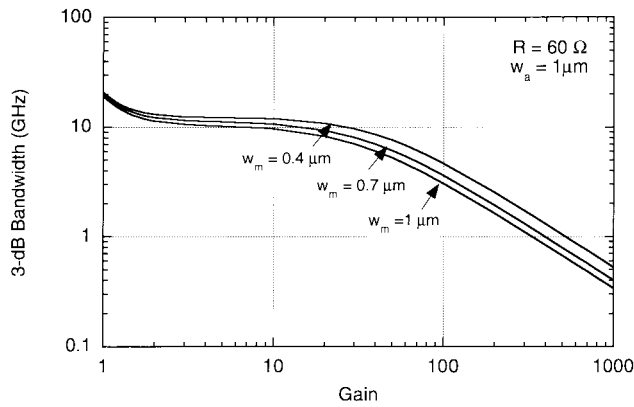


Fig. 10. Gain dependence of the 3-dB bandwidth for various values of the multiplication layer thickness and a constant electric field profile.

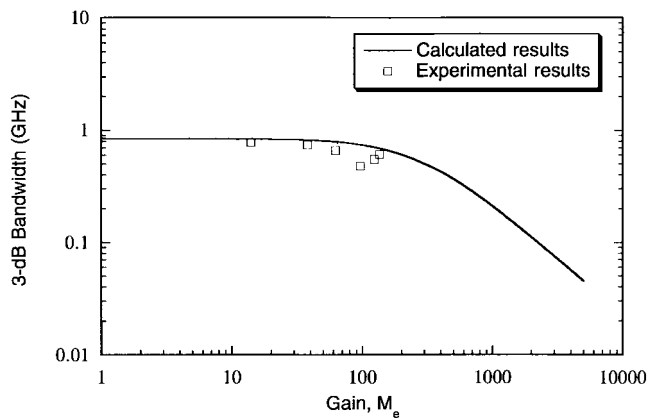


Fig. 11. 3-dB bandwidth as a function of the multiplication gain for a SHIP detector with  $w_a = 1 \mu\text{m}$ ,  $w_m = 2.5 \mu\text{m}$ . The resistance and the capacitance of the SHIP detector are  $2020 \Omega$  and  $0.1 \text{ pF}$ , respectively. The squares are the experimental data points while the solid line is the theoretical result.

The achievable gain-bandwidth product for different APD's under a uniform electric field profile can be calculated for different multiplication layer thicknesses. The dependence of the gain-bandwidth product on the thickness is shown in Fig. 13 for InGaAs/InP SAGM APD's, for superlattice APD's, and for InGaAs/InP SHIP APD's. The record experimental results are also shown for each structure. From Fig. 13, we can see that with  $w_a = 1 \mu\text{m}$ ,  $w_m = 0.4 \mu\text{m}$ , and a constant electric field profile, the gain-bandwidth product of a SHIP detector can be as high as 450 GHz, which is about three times as large as the recorded gain-bandwidth product for InGaAs/InP APD's [9].

## VI. CONCLUSION

The gain-bandwidth product is a very important figure for avalanche photodetectors. Currently, the gain-bandwidth product for the state-of-the-art InP/InGaAs APD's is around 150 GHz [9]. We have designed silicon hetero-interface photodetectors using silicon as the multiplication material and InGaAs as the absorption material. We have calculated the frequency response, gain-dependence of the 3-dB bandwidth, and quantum efficiencies for the SHIP detectors. Our calculated results show that the performance of a SHIP detector

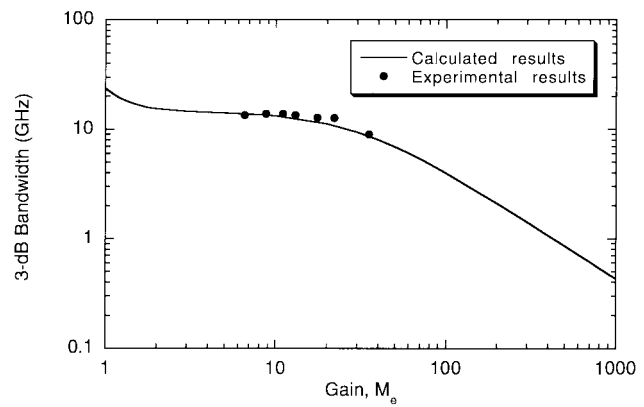


Fig. 12. 3-dB bandwidth as a function of the multiplication gain for a SHIP detector with  $w_a = 0.7 \mu\text{m}$ ,  $w_m = 0.6 \mu\text{m}$ .

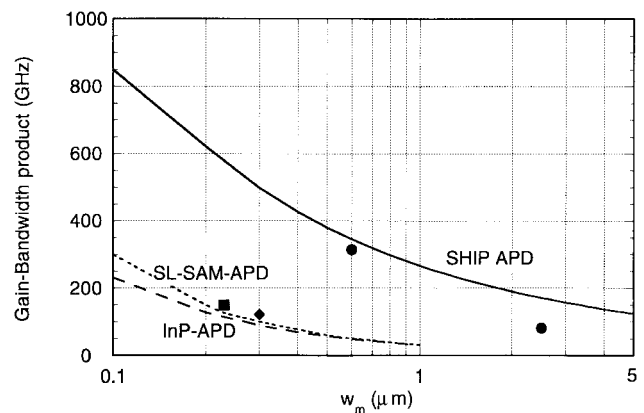


Fig. 13. Achievable gain-bandwidth product for SHIP detectors with uniform electric field profile as a function of the multiplication layer thickness. The circles are the measured gain-bandwidth products for SHIP APD's, while the squares are the best results for InGaAs/InP and superlattice APD's.

can be improved by properly selecting the thickness of the multiplication layer and the absorption layer. A SHIP detector with  $w_a = 1 \mu\text{m}$  and  $w_m = 0.4 \mu\text{m}$  should have a bandwidth of  $>10 \text{ GHz}$  and a gain-bandwidth product of 450 GHz, which will be very attractive for 10 Gbit/s high-speed optical communication systems. Bandwidths of 13 GHz and gain-bandwidth product of 315 GHz have been obtained.

## REFERENCES

- [1] J. C. Campbell, "Heterojunction photodetectors for optical communications," *Heterostructures and Quantum Devices*. New York: Academic, 1994, pp. 243–271.
- [2] L. Kasper and J. C. Campbell, "Multigigabit-per-second avalanche photodiode lightwave receivers," *J. Lightwave Technol.*, vol. LT-5, pp. 1351–1364, 1987.
- [3] S. Fujita, N. Henmi, I. Takano, M. Yamaguchi, T. Torikai, T. Suzuki, S. Takano, H. Ishihara, and M. Shikada, "A 10 Gbit/s 80 km optical fiber transmission experiment using a directly modulated DFB-LD and a high speed InGaAs APD," in *Tech. Dig. OFC'88*, New Orleans, LA, 1988, postdeadline paper.
- [4] R. B. Emmons, "Avalanche-photodiode frequency response," *J. Appl. Phys.*, vol. 38, pp. 3705–3714, 1967.
- [5] J. E. Bowers and C. A. Burrus, Jr., "Ultrawide-band long-wavelength *p-i-n* photodetectors," *J. Lightwave Technol.*, vol. LT-5, pp. 1339–1350, 1987.
- [6] S. R. Forrest, O. K. Kim, and R. G. Smith, "Optical response time of  $\text{In}_{0.53}\text{Ga}_{0.47}\text{As/InP}$  avalanche photodetectors," *Appl. Phys. Lett.*, vol. 41, pp. 95–98, 1982.

- [7] J. C. Campbell, W. T. Tsang, G. J. Qua, and J. E. Bowers, "InP/InGaAsP/InGaAs avalanche photodiodes with 70 GHz gain-bandwidth product," *Appl. Phys. Lett.*, vol. 51, pp. 1454–1456, 1987.
- [8] Y. K. Jhee, J. C. Campbell, J. F. Ferguson, A. G. Dentai, and W. S. Holden, "Avalanche buildup time of InP/InGaAsP/InGaAs avalanche photodiodes with separate absorption, grading, and multiplication regions," *IEEE J. Quantum Electron.*, vol. QE-22, pp. 753–755, 1986.
- [9] K. Makita, I. Watanabe, M. Tsuji, and K. Taguchi, "150 GHz GB-product and low dark current InAlGaAs quaternary well superlattice avalanche photodiodes," in *Tech. Dig. IOOC'95*, paper TuB2-1, 1995, pp. 36–37.
- [10] R. J. Ram, J. J. Dudley, J. E. Bowers, L. Yang, K. Carey, S. J. Rosner, and K. Nauka, "GaAs to InP wafer fusion," *J. Appl. Phys.*, vol. 78, pp. 4227–4237, 1995.
- [11] A. R. Hawkins, T. E. Reynolds, D. R. England, D. I. Babic, M. J. Mondry, K. Streubel, and J. E. Bowers, "Silicon hetero-interface photodetector," *Appl. Phys. Lett.*, vol. 68, pp. 3692–3694, 1996.
- [12] J. N. Hollenhorst, "Frequency response theory for multilayer photodiodes," *J. Lightwave Technol.*, vol. 8, pp. 531–537, 1990.
- [13] J. C. Campbell, B. C. Johnson, G. J. Qua, and W. T. Tsang, "Frequency response of InP/InGaAsP/InGaAs avalanche photodetectors," *J. Lightwave Technol.*, vol. 7, pp. 778–784, 1989.
- [14] W. Wu, A. R. Hawkins, and J. E. Bowers, "Frequency response of avalanche photodetectors with separate absorption and multiplication layers," *J. Lightwave Technol.*, vol. 15, pp. 2778–2785, Dec. 1996.
- [15] G. Kahraman, B. E. A. Saleh, W. L. Sargeant, and M. C. Teich, "Time and frequency response of avalanche photodiodes with arbitrary structure," *IEEE Trans. Electron Devices*, vol. 39, pp. 553–560, 1992.
- [16] W. N. Grant, "Electron and hole ionization rates in epitaxial silicon at high electric fields," *Solid-state Electron.*, vol. 16, pp. 1189–1203, 1973.
- [17] R. J. McIntyre, "Multiplication noise in uniform avalanche diodes," *IEEE Trans. Electron Devices*, vol. ED-13, pp. 164–168, 1966.
- [18] R. Kuvass and C. A. Lee, "Quasistatic approximation for semiconductor avalanche," *J. Appl. Phys.*, vol. 41, pp. 1743–1755, 1970.
- [19] W. Wu, A. R. Hawkins, and J. E. Bowers, "Gain-bandwidth products of avalanche photodetectors," *IEEE Photon. Technol. Lett.*, to be published.
- [20] P. P. Webb, "Measurement of ionization coefficients in silicon at low electric fields," GE Canada Inc.
- [21] L. W. Cook, G. E. Bulman, and G. E. Stillman, "Electron and hole ionization coefficients in InP determined by photomultiplication measurements," *Appl. Phys. Lett.*, vol. 40, pp. 589–591, 1982.
- [22] T. P. Pearsall, "Impact ionization rates for electrons and holes in Ga<sub>0.47</sub>In<sub>0.53</sub>As," *Appl. Phys. Lett.*, vol. 36, pp. 218–220, 1980.
- [23] H. D. Law and C. A. Lee, "Interband scattering effects on secondary ionization coefficients in GaAs," *Solid-State Electron.*, vol. 21, pp. 331–340, 1978.
- [24] C. A. Lee, R. A. Logan, R. L. Batdorf, J. J. Kleimack, and W. Wiegmann, "Ionization rates of hole and electrons in silicon," *Phys. Rev.*, vol. 134, pp. A761–773, 1964.
- [25] T. Kaneda, H. Matsumoto, and T. Yamaoka, "A model for reach-through avalanche photodiodes (RAPD's)," *J. Appl. Phys.*, vol. 47, pp. 3135–3139, 1976.
- [26] R. J. McIntyre, "Recent developments in silicon avalanche photodiodes," *Measurement*, vol. 3, pp. 146–152, 1985.
- [27] A. R. Hawkins, W. Wu, P. Abraham, K. Streubel, and J. E. Bowers, "High gain-bandwidth-product silicon heterointerface photodetector," *Appl. Phys. Lett.*, vol. 70, 1997.
- Weishu Wu**, photograph and biography not available at the time of publication.
- Aaron R. Hawkins**, photograph and biography not available at the time of publication.
- John E. Bowers**, photograph and biography not available at the time of publication.